JVI Journals.ASM.org

Apoptosis Induced by Mammalian Reovirus Is Beta Interferon (IFN) Independent and Enhanced by IFN Regulatory Factor 3- and NF-κB-Dependent Expression of Noxa

Jonathan J. Knowlton,[a] Terence S. Dermody,[b,c,d] and Geoffrey H. Holm[a]

Department of Biology, Colgate University, Hamilton, New York, USA,[a] and Departments of Pediatrics[b] and Pathology, Microbiology, and Immunology,[c] and the Elizabeth B. Lamb Center for Pediatric Research,[d] Vanderbilt University School of Medicine, Nashville, Tennessee, USA

A variety of signal transduction pathways are activated in response to viral infection, which dampen viral replication and transmission. These mechanisms involve both the induction of type I interferons (IFNs), which evoke an antiviral state, and the triggering of apoptosis. Mammalian orthoreoviruses are double-stranded RNA viruses that elicit apoptosis *in vitro* and *in vivo*. The transcription factors interferon regulatory factor 3 (IRF-3) and nuclear factor kappa light-chain enhancer of activated B cells (NF-κB) are required for the expression of IFN-β and the efficient induction of apoptosis in reovirus-infected cells. However, it is not known whether IFN-β induction is required for apoptosis, nor have the genes induced by IRF-3 and NF-κB that are responsible for apoptosis been identified. To determine whether IFN-β is required for reovirus-induced apoptosis, we used type I IFN receptor-deficient cells, IFN-specific antibodies, and recombinant IFN-β. We found that IFN synthesis and signaling are dispensable for the apoptosis of reovirus-infected cells. These results indicate that the apoptotic response following reovirus infection is mediated directly by genes responsive to IRF-3 and NF-κB. Noxa is a proapoptotic BH3-domain-only protein of the Bcl-2 family that requires IRF-3 and NF-κB for efficient expression. We found that Noxa is strongly induced at late times (36 to 48 h) following reovirus infection in a manner dependent on IRF-3 and NF-κB. The level of apoptosis induced by reovirus is significantly diminished in cells lacking Noxa, indicating a key prodeath function for this molecule during reovirus infection. These results suggest that prolonged innate immune response signaling induces apoptosis by eliciting Noxa expression in reovirus-infected cells.

The innate immune system provides vital early defenses against viral infections. At the cellular level, responses to virus entry often dictate the outcome of infection and the subsequent likelihood of virus dissemination past the point of initial contact. Cytoplasmic restriction factors can suppress the capacity of viruses to replicate and function as a first line of defense. If these mechanisms fail, cells may take more costly steps to eradicate infection by inducing the type I interferon (IFN) pathway. Beta interferon (IFN-β) secreted by infected cells enhances the expression of many antiviral interferon-stimulated genes (ISGs), which can prevent viral replication by degrading RNAs and inhibiting protein synthesis. However, these mechanisms come at the expense of halting cellular protein synthesis and can compromise cell viability. A final, much more drastic outcome is the induction of apoptosis, which sacrifices infected cells but may spare uninfected surrounding cells. While antiviral restriction factors may be synthesized constitutively, both the IFN and apoptosis pathways are tightly regulated to prevent untoward effects of inappropriate antiviral activity.

Cytoplasmic sensors of virus-specific molecular patterns, including double-stranded RNA (dsRNA), initiate transcriptional responses to infection. The retinoic acid-inducible gene I (RIG-I)-like helicases (RLHs) RIG-I and melanoma differentiation-associated gene 5 (Mda5) bind dsRNA in the cytoplasm (38, 80, 91) and activate beta interferon promoter stimulator 1 (IPS-1/MAVS/VISA/Cardif) (39, 53, 71, 90). IPS-1 subsequently engages the kinases inhibitor of κB kinase alpha (IKK-α), IKK-β, IKK-ε, and Tank-binding kinase 1 (TBK1), which activate transcription factors, including activating transcription factor 2 (ATF-2)/c-Jun, IFN regulatory factor 3 (IRF-3), and NF-κB (53, 71, 90). Once in the nucleus, these transcription factors induce the expression of a variety of inflammatory and antiviral genes, including IFN-β (58, 68).

Type I IFNs initiate a second cellular transcriptional response following the engagement of the IFN-α/β receptor (IFNAR) (reviewed in reference 13). The receptor signals through a JAK/STAT pathway to activate a heterotrimeric transcriptional complex, termed interferon-stimulated gene factor 3 (ISGF3). This complex, which contains phosphorylated STAT1 and STAT2 along with IRF-9, translocates to the nucleus and binds to interferon-stimulated response elements (ISREs) located in the promoters of hundreds of ISGs. One such ISG is IRF-7, which can homodimerize or heterodimerize with IRF-3 to further upregulate type I IFNs in a positive-feedback loop (50). Other ISGs exert antiviral effects through a variety of different mechanisms. For example, protein kinase R (PKR) is activated by dsRNA and phosphorylates the alpha subunit of eukaryotic initiation factor 2 (eIF2α), blocking translation initiation (61). The enzyme 2′-5′-oligoadenylate synthase (2′5′OAS) also is activated by dsRNA to produce 2′-5′-adenylic acid, which stimulates RNase L to degrade cellular RNA (11). These and other mechanisms prevent virus replication in infected cells and prime neighboring cells to enter a refractory antiviral state.

Received 9 August 2011 **Accepted** 9 November 2011
Published ahead of print 16 November 2011
Address correspondence to Geoffrey H. Holm, gholm@colgate.edu.

doi:10.1128/JVI.05924-11

Several ISGs are capable of initiating or facilitating proapoptotic signaling. PKR can induce apoptosis following viral infection (5, 51, 84), although the effects are cell type and virus specific (92). ISG54 (IFIT2) and ISG12b2 also mediate proapoptotic functions (49, 77). Additionally, components of extrinsic apoptosis signaling pathways, such as tumor necrosis factor alpha (TNF-α)-related apoptosis-inducing ligand (TRAIL/Apo2L), Fas, and Fas-associated death domain (FADD), are linked to IFN-dependent apoptosis (5, 40, 70). FADD is involved in signaling via IPS-1, suggesting that it may bridge pre-IFN-induction and post-IFN-induction signaling events (39). A complicating factor for many of these studies is that some of these ISGs, including ISG54, can be induced directly by IRF-3 (2), making the requirement for IFN-mediated signaling in these apoptotic pathways difficult to delineate. Nonetheless, it is apparent that cellular innate immune processes are intricately linked to the apoptotic machinery.

Mammalian orthoreoviruses (reoviruses) cause apoptosis-associated encephalitis and myocarditis in infected newborn mice (26, 55). As such, these viruses are useful model pathogens for studies of cell death signaling following virus infection. Reoviruses also efficiently lyse tumor cells in experimental animals (19, 29) and show efficacy in clinical trials for aggressive and refractory human tumors (78, 85). Reovirus particles are nonenveloped and encapsidate a genome of 10 dsRNA segments (69). Following internalization into host cells, reoviruses are detected by RIG-I and Mda-5, which in turn lead to the activation of IRF-3 and NF-κB (20, 35, 48). In keeping with the linkage between antiviral innate immunity and apoptotic cell death, both IRF-3 and NF-κB are required for maximum levels of apoptosis in response to reovirus (20, 35). Many cellular proapoptotic factors, including Bid, Bax, TRAIL, and Fas, also enhance apoptosis in reovirus-infected cells (9, 15, 18, 24). However, mechanisms by which these proteins become activated, and the specific functions of IRF-3 and NF-κB in this process, remain unclear. Reovirus mutants that induce diminished levels of apoptosis display attenuated virulence in the murine central nervous system (CNS), indicating a predominant role for apoptosis in reovirus pathogenicity (22, 23). This conclusion is strengthened by the finding that reovirus neurovirulence is diminished in NF-κB p50-deficient mice (57). However, these effects are likely cell or tissue type dependent, as reovirus induces severe myocarditis in mice that lack either IRF-3 or NF-κB p50 (36, 57).

Despite experimental evidence linking IRF-3 and NF-κB to reovirus-induced apoptosis, the IRF-3- and NF-κB-dependent genes responsible for initiating this cell death mechanism are not known with certainty. Microarray studies of gene expression following reovirus infection revealed that several ISGs are rapidly upregulated following infection in an NF-κB-dependent manner (58). However, those studies did not identify a mediator of proapoptotic signaling that could readily explain the cell death pathways initiated by reovirus infection. Given previous studies of IFN-mediated apoptosis, we sought to determine whether reovirus-induced cell death requires IFN signaling and, if not, identify which IRF-3- or NF-κB-dependent genes might elicit apoptosis in an IFN-independent manner. We found that IFN signaling, and, thus, IFN-dependent ISG transcription, is not required for the triggering of apoptosis in reovirus-infected cells. We also identified a role for the IRF-3- and NF-κB-dependent regulation of Noxa, a proapoptotic BH3-domain-only protein of the Bcl-2 family (56), as an effector of reovirus-induced apoptosis. Remarkably, despite its dependence on IRF-3 and NF-κB, which are first activated 2 to 4 h postinfection, Noxa was upregulated at late times (36 to 48 h) postinfection. These results suggest that prolonged innate immune activation, perhaps in the absence of an effective IFN-mediated antiviral response, may result in cell death as a final defense against prolonged virus replication.

MATERIALS AND METHODS

Cells and viruses. Mouse embryo fibroblasts (MEFs) and 293T cells were maintained in Dulbecco's modified Eagle's medium supplemented to contain 10% fetal bovine serum, 2 mM L-glutamine, 100 units/ml of penicillin, 100 μg/ml streptomycin, and 25 ng/ml of amphotericin B (Invitrogen). L929 cells were maintained in Joklik's minimum essential medium supplemented to contain 5% fetal bovine serum, 2 mM L-glutamine, 100 units/ml of penicillin, 100 μg/ml streptomycin, and 25 ng/ml of amphotericin B. MEFs deficient in IRF-3 and matched wild-type controls (68) were obtained from Karen Mossman. MEFs deficient in IFNAR and matched wild-type controls (54) were obtained from H. W. Virgin and Christian Schindler (93). MEFs deficient in Noxa and matched wild-type controls (87) were obtained from Navdeep Chandel. MEFs deficient in NF-κB p65 and matched wild-type controls (8) were obtained from David Baltimore.

Reovirus strain type 3 Dearing (T3D) is of a laboratory stock. Purified reovirus virions were generated by using second- or third-passage L-cell lysate stocks of twice-plaque-purified reovirus as described previously (31). Viral particles were Freon extracted from infected cell lysates, layered onto 1.2- to 1.4-g/cm^3 CsCl gradients, and centrifuged at 62,000 $\times$ *g* for 18 h. Bands corresponding to virions (1.36 g/cm^3) (76) were collected and dialyzed in virion storage buffer (150 mM NaCl, 15 mM $MgCl_2$, 10 mM Tris-HCl [pH 7.4]). The viral titer was determined by a plaque assay using murine L929 cells (88).

Assays of virus growth. MEFs (2×10^4) grown in 24-well plates were adsorbed in triplicate with T3D in serum-free medium at various multiplicities of infection (MOIs) at 25°C for 1 h, washed once with phosphate-buffered saline (PBS), and incubated in serum-containing medium for various intervals. The cells were frozen and thawed three times, followed by the determination of viral titers by a plaque assay using L929 cells. Viral yields were calculated according to the following formula: $\log_{10}\text{yield}t_x = \log_{10}(\text{PFU/ml})t_x - \log_{10}(\text{PFU/ml})t_0$, where t_x is the time postinfection.

Quantification of apoptosis by acridine orange staining. MEFs (5×10^4) grown in 24-well plates were either mock infected or adsorbed with T3D in serum-free medium at various MOIs at 25°C for 1 h. Staurosporine (STS) (1 μM; Sigma-Aldrich) was used as a positive control and administered 16 h before analysis. Following 48 h of incubation in serum-containing medium, the percentage of apoptotic cells was determined by using acridine orange staining as described previously (86). For each experiment, >200 cells were counted, and the percentage of cells exhibiting condensed chromatin was determined by epi-illumination fluorescence microscopy using a fluorescein filter set (Photomicroscope III; Zeiss, New York, NY). To control for differences in the percentages of apoptotic cells observed following reovirus infection of the different wild-type MEF cell lines, the percentage of apoptotic cells was normalized to the average percentage of apoptotic cells induced by T3D in the wild-type MEFs used in each experiment.

Detection of caspase-3/7 activity. MEFs (5×10^3) seeded into black clear-bottom 96-well plates were either adsorbed with T3D in serum-free medium at various MOIs at 25°C for 1 h or treated with STS (1 μM) as a positive control 5 h prior to analysis. Following various intervals of incubation in serum-containing medium, caspase-3/7 activity was quantified by using the Caspase-Glo 3/7 assay (Promega) according to the manufacturer's instructions.

Type I IFN treatment and antibody blockade. IRF-3$^{+/+}$ or IRF-3$^{-/-}$ MEFs (5×10^4) grown in 24-well plates were inoculated with PBS or reovirus T3D at an MOI of 100 PFU/cell at 4°C for 45 min. The inoculum was removed, and cells were incubated in Dulbecco's modified Eagle's

medium (DMEM) in the presence or absence of either rabbit anti-mouse IFN-β polyclonal IgG (Calbiochem, EMD Chemicals, Gibbstown, NJ) at a concentration of 500 neutralization units (NU)/ml or recombinant mouse IFN-β (Calbiochem) at a concentration of 50 international units (IU)/ml. Cell death was quantified by acridine orange staining at 48 h postinfection.

Immunoblot assay. 293T cells (5×10^5) grown in 60-mm dishes were adsorbed with T3D in serum-free medium at an MOI of 100 PFU/cell at 25°C for 1 h. Cells were incubated in serum-containing medium at 37°C for various intervals, removed from plates with a scraper, washed once with PBS, and centrifuged at $500 \times g$ for 5 min. Whole-cell extracts were prepared by incubation in radioimmunoprecipitation assay (RIPA) lysis buffer (50 mM Tris HCl [pH 7.4], 1% NP-40, 0.25% sodium deoxycholate, 150 mM NaCl) containing a cocktail of protease inhibitors (catalog number 04693124001; Roche) on ice for 5 min, followed by centrifugation at $10{,}000 \times g$ for 10 min to remove cellular debris. Extracts were resolved by electrophoresis in 12% polyacrylamide gels and transferred onto polyvinylidene difluoride (PVDF) membranes. Membranes were blocked at room temperature overnight in blocking buffer (PBS containing 0.1% Tween 20 and 2% bovine serum albumin). Immunoblots were performed by the incubation of membranes with a monoclonal mouse anti-Noxa primary antibody (ab13654; Abcam) diluted 1:500 in blocking buffer for 2 h. Membranes were washed 3 times for 10 min each with washing buffer (PBS containing 0.1% Tween 20) and incubated with an alkaline phosphatase-conjugated goat anti-mouse secondary antibody (kit number 170-5010; Bio-Rad) diluted 1:1,000 in blocking buffer for 2 h. After three washes, membranes were incubated for 5 min with chemiluminescent alkaline phosphatase substrate (Bio-Rad). Protein bands were visualized by using a Bio-Rad ChemiDoc XRS$^+$ molecular imager, and the band intensity was quantified by using the Image J program.

Quantitative reverse transcriptase PCR. 293T cells or MEFs (5×10^5) grown in 60-mm dishes were adsorbed with T3D in serum-free medium at an MOI of 100 PFU/cell at 25°C for 1 h. Cells were incubated in serum-containing medium at 37°C for various intervals, removed from plates with a scraper, washed once with PBS, and centrifuged at $500 \times g$ for 5 min. The supernatant was removed, and the cell pellet was frozen at −20°C. RNA was extracted by using an RNeasy Plus RNA extraction minikit (Qiagen) according to the manufacturer's instructions. RNA was converted to by cDNA by using an Omniscript RT cDNA synthesis kit (Qiagen) with an oligo(dT) primer or a reovirus L1 minus-strand-specific primer (5′-GGGCTCTATGCTGTGCTTTC-3′) according to the manufacturer's instructions. Quantitative PCR (qPCR) was performed by using the Express SYBR GreenER system (Invitrogen). Primers specific for the following RNA transcripts were used at a concentration of 0.2 μM: mouse glyceraldehyde-2-phosphate dehydrogenase (GAPDH) (forward [F] primer 5′-ACCCAGAAGACTGTGGATGG-3′ and reverse [R] primer 5′-GGATGCAGGGATGATGTTCT-3′), human GAPDH (F primer 5′-GATCATCAGCAATGCCTCCT-3′ and R primer 5′-TGTGGTCATGAGTCCTTCCA-3′), mouse Noxa (F primer 5′-CCCAGATTGGGGACCTTAGT-3′ and R primer 5′-CTGCGAACTCAGGTGGTAGC-3′), human Noxa (F primer 5′-GAGATGCCTGGGAAGAAGG-3′ and R primer 5′-TTCTGCCGGAAGTTCAGTTT-3′), IFIT1 (F primer 5′-GCAACCATGGGAGAGAATG-3′ and R primer 5′-CCCAATGGGTTCTTGATGTC-3′), interleukin-6 (IL-6) (F primer 5′-CCGGAGAGGAGACTTCACAG-3′ and R primer 5′-CAGAATTGCCATTGCACAAC-3′), and reovirus L1 (Reo L1) (F primer 5′-GGGCTCTATGCTGTGCTTTC-3′ and R primer 5′-GGGCGTATCAAGCTAATCCA-3′). Quantification and melt curve analyses were performed according to the manufacturer's protocol. For each sample, the C_T (threshold cycle) for the RNA of interest was normalized to that for GAPDH. Fold induction was calculated by comparing normalized C_T values ($\Delta\Delta C_T$) of duplicate cDNA synthesis reactions to those of samples taken at the time of infection ($T = 0$) for three independent experiments. For the quantification of reovirus L1 gene segments, samples were normalized to GAPDH expression levels in matched cDNA synthesized by using an oligo(dT) primer.

Silencing of Noxa expression by RNA interference (RNAi). 293T cells (10^6) grown in 60-mm dishes overnight were transfected with 100, 200, or 400 pmol control or Noxa (PMAIP1)-specific small interfering RNAs (siRNAs) (PMAIP1HSS143342 and PMAIP1HSS143343; Invitrogen) by using Lipofectamine 2000 (Invitrogen) according to the manufacturer's instructions. To confirm the knockdown of Noxa mRNA and protein, qPCR and immunoblotting were performed as described above at 24 h posttransfection. For experiments to address the function of Noxa in apoptosis, cells in 60-mm dishes were transfected with 200 pmol control or Noxa-specific siRNAs and replated in 24-well plates (8×10^4 cells/well) at 24 h posttransfection. Following an additional 12 h of incubation, cells were retransfected with 20 pmol Noxa-specific or control siRNAs and incubated for 12 h. Cells were either mock infected or adsorbed with T3D in serum-free medium at an MOI of 100 PFU/cell at 25°C for 1 h. Following 48 h of incubation in serum-containing medium, the percentage of apoptotic cells was determined by using acridine orange staining.

Statistics. Statistical analyses were performed by using GraphPad Prism software.

RESULTS

Type I IFN receptor signaling inhibits reovirus spread in tissue culture. Efficient apoptosis induction following reovirus infection is dependent on the transcription factors IRF-3 and NF-κB (20, 34, 35). Despite this association, microarray analysis of NF-κB-dependent genes induced following reovirus infection did not identify a readily apparent mechanism for the initiation of apoptosis (58). However, a number of transcriptional networks that couple to apoptotic signaling pathways were identified. Most prominent among these was a large number of ISGs strongly upregulated at 6 to 10 h postinfection. Since IFN signaling is linked to apoptosis induction in several other virus infection models (5, 59, 83), we examined the role of type I IFNs and IFN-dependent signaling in reovirus replication and apoptosis.

Type I IFNs have pleiotropic effects on host cells (82). To distinguish between effects on replication and effects on apoptosis, we first examined the effect of IFN signaling on reovirus replication. For these experiments, we used MEFs derived from animals genetically lacking IFNAR (54). We quantified titers of reovirus T3D over a single cycle of viral replication following infection at an MOI of 10 PFU/cell. Yields of T3D in IFNAR$^{+/+}$ and IFNAR$^{-/-}$ MEFs at 24 or 48 h postinfection did not differ (Fig. 1A). Thus, IFN signaling has little effect on reovirus growth during a single replication cycle. To determine whether IFN signaling limits the capacity of reovirus to spread in cell culture during multiple rounds of infection, we infected IFNAR$^{+/+}$ or IFNAR$^{-/-}$ MEFs at an MOI of 1 PFU/cell and quantified viral titers over a time course of 5 days. At days 4 and 5 postinfection, reovirus reached 10- to 50-fold-higher yields in IFNAR$^{-/-}$ MEFs than in IFNAR$^{+/+}$ MEFs (Fig. 1B). Therefore, similar to our previously reported observations using IRF-3-deficient MEFs (35), type I IFNs limit the capacity of reovirus to spread to uninfected cells in an infected culture.

IFN-β is dispensable for apoptosis caused by reovirus. We next assessed the role of IFN-β in inducing apoptosis following reovirus infection using three independent approaches. First, we assessed the capacity of anti-IFN-β neutralizing antibodies to inhibit apoptosis in MEFs. Wild-type and IRF-3$^{-/-}$ MEFs were infected with T3D at an MOI of 100 PFU/cell. At the time of infection, cultures were mock treated or treated with neutralizing anti-IFN-β antibodies at a concentration of 500 NU/ml. This concentration is 10-fold higher than that which is sufficient to neu-

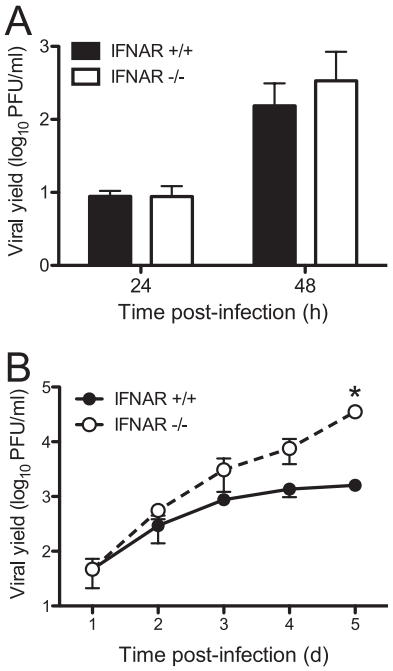

FIG 1 Reovirus spread is diminished by type I IFN signaling. IFNAR$^{+/+}$ MEFs and IFNAR$^{-/-}$ MEFs were infected with T3D at an MOI of 10 PFU/cell (A) or 1 PFU/cell (B). Titers of infectious virus in cell lysates at the indicated times postinfection were determined by a plaque assay. The results are expressed as viral yields for triplicate samples. The error bars indicate standard deviations (SD). The asterisk indicates differences in viral yield in each cell line that are significant ($P < 0.001$), as determined by two-way analysis of variance (ANOVA).

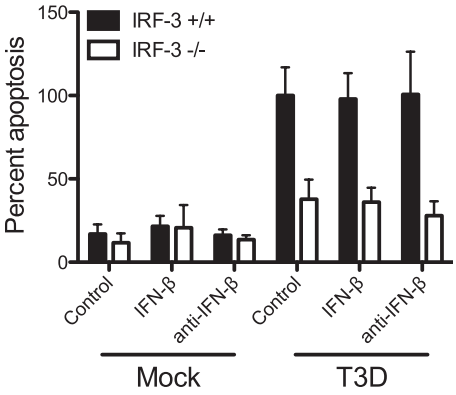

FIG 2 IFN-β does not potentiate apoptosis following reovirus infection. IRF-3$^{+/+}$ MEFs and IRF-3$^{-/-}$ MEFs were mock infected or infected with T3D at an MOI of 100 PFU/cell. At the time of infection, cultures were mock treated or treated with either IFN-β-specific neutralizing antibodies or recombinant IFN-β. Following 48 h of incubation, the percentage of apoptotic cells was determined after staining with acridine orange. The results are expressed as the mean percentages of apoptotic cells for triplicate samples, normalized to the average percentage of apoptotic cells in T3D-infected IRF-3$^{+/+}$ MEFs. The error bars indicate SD.

tralize IFN-β produced by wild-type MEFs following reovirus infection (35). After 48 h, the percentage of apoptotic cells in the cultures was determined following acridine orange staining, which allows the identification of apoptotic cells by morphological criteria. Acridine orange staining is an established technique to quantify levels of apoptosis induced by reovirus (20, 21, 35, 86). Treatment with neutralizing antibodies against IFN-β did not inhibit apoptosis induced by reovirus in wild-type MEFs (Fig. 2). We next assessed the capacity of exogenous IFN-β to induce apoptosis following reovirus infection of IRF-3-deficient MEFs. These cells respond to IFN-β but do not produce this cytokine following reovirus infection (35). At the time of infection, wild-type or IRF-3$^{-/-}$ cultures were mock treated or treated with recombinant mouse IFN-β at a concentration of 50 IU/ml, which is approximately 10-fold higher than the amount of IFN-β produced following reovirus infection of wild-type MEFs (35). Apoptosis induction was assessed following acridine orange staining at 48 h postinfection. Recombinant IFN-β did not increase the percentage of apoptotic cells in either wild-type or IRF-3-deficient cultures (Fig. 2). The efficacy of anti-IFN-β neutralizing antibody and exogenous IFN-β treatments was confirmed by qPCR measurements of the induction of an ISG, IFIT1, in cells treated with IFN-β in the presence or absence of IFN-β-neutralizing antibodies. As expected, IFN-β treatment increased the level of expression of IFIT1 in both wild-type and IRF-3$^{-/-}$ MEFs, which was abrogated in the presence of anti-IFN-β neutralizing antibodies (data not shown). Finally, we determined whether reovirus is capable of inducing apoptosis in IFNAR-deficient cells, which cannot respond to IFN-β. IFNAR$^{+/+}$ and IFNAR$^{-/-}$ MEFs were infected with T3D at an MOI of 100 PFU/cell, and apoptosis was assessed by caspase-3/7 activity, an indicator of the effector phase of apoptosis, at 24 h postinfection and by acridine orange staining at 48 h postinfection. No differences were observed between IFNAR$^{+/+}$ and IFNAR$^{-/-}$ MEFs in either caspase-3/7 activity (Fig. 3A) or acridine orange staining (Fig. 3B) following reovirus infection. Collectively, these data suggest that IFN-β expression and signaling are not required for reovirus-induced apoptosis. Therefore, although IRF-3 and NF-κB are required for IFN induction and apoptosis initiation, independent pathways appear to evoke these cellular responses.

Noxa expression is upregulated following reovirus infection in an IRF-3- and NF-κB-dependent manner. In attempting to identify a candidate protein that is a transcriptional target of IRF-3 or NF-κB that facilitates that apoptosis of reovirus-infected cells, we thought that this protein would act via the intrinsic apoptotic pathway, since this pathway could function entirely intracellularly. Additionally, reovirus apoptosis is mediated at least in part via intrinsic apoptotic signals, leading to the release of cytochrome *c* and Smac/Diablo from mitochondria (42, 43). The intrinsic mechanism of apoptosis is induced by BH3-domain-only proteins of the Bcl-2 family via the inhibition of antiapoptotic Bcl-2 family members located in the mitochondrial membrane (79). Based on these observations, we reasoned that Noxa, a proapoptotic BH3-domain-only protein (56) regulated by IRF-3 (32, 45) and NF-κB (37, 60), might be required for reovirus-induced apoptosis. In support of this idea, Noxa is implicated in apoptosis following infection with encephalomyocarditis virus (ECMV), Sendai virus, vaccinia virus (modified Ankara strain), and vesicular stomatitis virus (VSV) (30, 32, 45, 81). Since Noxa expression is controlled at the transcriptional level, we first examined whether Noxa mRNA expression is induced following reovirus infection. 293T cells were infected with T3D, and RNA was extracted from mock-infected and infected cultures at various times postinfection. Levels of Noxa mRNA were quantified by using qPCR. We observed a continuous, time-dependent increase in Noxa expression levels fol-

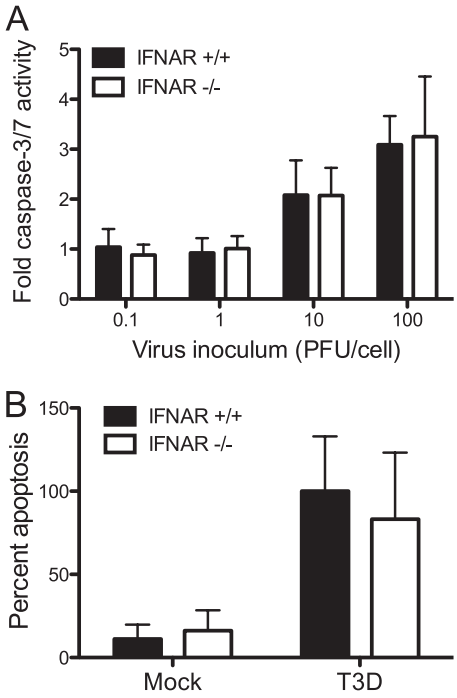

FIG 3 IFN signaling is not required for induction of apoptosis by reovirus. IFNAR$^{+/+}$ MEFs and IFNAR$^{-/-}$ MEFs were infected with T3D at the indicated MOIs. (A) Caspase-3/7 activity in cell lysates was determined at 24 h postinfection. The results are expressed as the mean ratios of caspase-3/7 activity from infected cell lysates to that from mock-infected cells for triplicate samples. The error bars indicate SD. (B) The percentage of apoptotic cells was determined after staining with acridine orange at 48 h postinfection. The results are expressed as the mean percentages of apoptotic cells for triplicate samples, normalized to the average percentage of apoptotic cells in T3D-infected IFNAR$^{+/+}$ MEFs. The error bars indicate SD.

lowing T3D infection. Noxa expression levels in these cells increased over 20-fold from baseline levels by 48 h postinfection (Fig. 4A). The levels of the Noxa protein showed a similar increase following reovirus infection, as determined by the immunoblotting of 293T cell lysates using a Noxa-specific antiserum (Fig. 4B and C).

To determine whether Noxa induction is IRF-3 or NF-κB dependent, wild-type, IRF-3$^{-/-}$, and NF-κB p65$^{-/-}$ MEFs were infected with T3D, and levels of Noxa mRNA were quantified by using qPCR. In wild-type MEFs, the Noxa expression level was increased over 6-fold from baseline levels by 48 h postinfection (Fig. 4D). In contrast, no significant upregulation of Noxa was observed following infection of IRF-3- or NF-κB p65-deficient MEFs. As a control for the efficacy of reovirus induction of transcriptional activity in these cell lines, we examined the expression of IL-6 and IFIT1 in these cell lines following reovirus infection. IL-6 expression is regulated by NF-κB (47), whereas IFIT1 is regulated by IRF-3 (33). As expected, IL-6 was induced following the infection of IRF-3-deficient MEFs, and IFIT1 was induced following the infection of NF-κB p65-deficient MEFs, suggesting that these cells were efficiently infected with reovirus and that signaling downstream of RIG-I and Mda-5 was intact despite the genetic deficiency in either IRF-3 or NF-κB (Fig. 4E and F).

Noxa expression does not affect reovirus replication. To determine whether Noxa expression alters reovirus replication, we utilized MEFs derived from Noxa$^{-/-}$ mice (87). Wild-type and Noxa-deficient MEFs were infected with T3D at an MOI of 1 PFU/cell, and viral yields were determined at 24 and 48 h postinfection. T3D produced equivalent yields in wild-type and Noxa$^{-/-}$ MEFs (Fig. 5A), suggesting that Noxa expression does not alter the capacity of reovirus to replicate. As the level of reovirus RNA synthesis may influence apoptosis induction via the activation of RIG-I- and Mda-5-dependent signaling, we also assessed the level of negative-strand synthesis in wild-type and Noxa$^{-/-}$ MEFs using qPCR with primers specific for the L1 gene segment. T3D produced equivalent levels of L1 negative-strand RNA in wild-type and Noxa$^{-/-}$ MEFs (Fig. 5B), suggesting that Noxa does not alter reovirus polymerase activity and, therefore, the amount of viral RNA capable of eliciting a signal via RIG-I and Mda-5.

Noxa is required for efficient apoptosis induction following reovirus infection. To determine whether Noxa influences apoptosis following reovirus infection, we quantified levels of apoptosis in wild-type and Noxa-deficient MEFs after mock infection or infection with T3D. As Noxa expression leads to caspase-3 activation via the intrinsic pathway of apoptosis, we first assessed caspase-3/7 activity over a time course following infection. STS was used as a positive control. Noxa$^{-/-}$ MEFs displayed significantly lower levels of caspase-3/7 activity following infection with T3D than did wild-type MEFs at 24, 36, and 48 h postinfection ($P < 0.05$) (Fig. 6A). In contrast, no significant difference in levels of caspase-3/7 induced in wild-type or Noxa$^{-/-}$ cells was observed following STS treatment (Fig. 6B). Similar results were obtained following the quantification of apoptosis in wild-type and Noxa$^{-/-}$ MEFs via acridine orange staining ($P < 0.05$) (Fig. 6C).

To confirm a role for Noxa in reovirus-induced apoptosis, we used RNAi to selectively diminish the expression level of Noxa and then quantified levels of apoptosis in infected cells. 293T cells were transfected with Noxa-specific siRNAs or a control siRNA, infected with T3D, and scored for apoptosis 48 h after infection by using acridine orange staining. Cells transfected with Noxa-specific siRNAs exhibited significantly diminished levels of apoptosis in comparison to those of cells transfected with control siRNA ($P < 0.05$) (Fig. 6D). The Noxa expression level was efficiently diminished following siRNA treatment, as assessed by the immunoblotting of transfected cell lysates with an antiserum specific for Noxa (Fig. 6E and F) and by qPCR analysis of total mRNA extracted from transfected cells using Noxa-specific primers (Fig. 6G). Together with results gathered using Noxa$^{-/-}$ MEFs, these findings indicate a critical function for Noxa in the efficient induction of apoptosis by reovirus.

DISCUSSION

At the center of the cellular innate immune response to virus infection is the decision of whether or not to undergo apoptosis. If the antiviral machinery can successfully clear the pathogen, normal cellular functions may be restored. However, if virus replication is unchecked, or if the damage caused by infection is too great, apoptosis may hinder further replication or facilitate the immune clearance of infected cells. This decision requires the capacity for the detection of products of viral infection by cellular pattern recognition receptors (PRRs) and a regulatory network capable of eliciting the appropriate response. Signals induced by PRRs engage a range of transcriptional circuits that regulate antiviral and apoptotic activities. Although many of the individual components of these circuits are known, how these signals are integrated to coordinate the response is less well understood. In this study, we

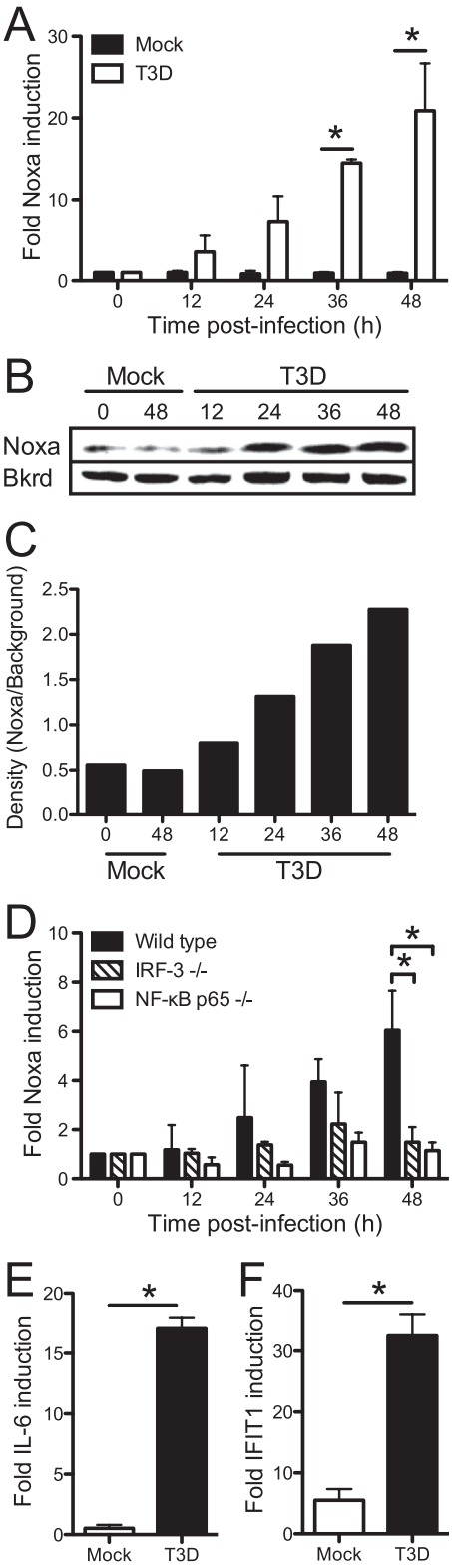

FIG 4 Reovirus-induced Noxa upregulation is dependent on IRF-3 and NF-κB p65. (A to D) 293T cells (A to C) and wild-type, IRF-3$^{-/-}$, and NF-κB p65$^{-/-}$ MEFs (D) were infected with T3D at an MOI of 100 PFU/cell. Levels of Noxa mRNA were quantified by using qPCR (A and D) or immunoblotting of cell lysates with an antiserum specific for Noxa (B and C) at the indicated times postinfection. In panel C, the Noxa-specific band intensity (Noxa) in panel B was quantified by using densitometry measurements and normalized to the intensity of a nonspecific background band (Bkrd). (E and F) Expression of IL-6 (E) or IFIT1 (F) in mock-infected or T3D-infected IRF-3$^{-/-}$ or NF-κB$^{-/-}$ MEFs, respectively, was determined at 48 h postinfection. For qPCR experiments, the gene-specific expression level was normalized to the GAPDH expression level. The results are expressed as the mean fold increases in the gene expression level relative to the expression level at the time of infection for three independent experiments with duplicate samples. The error bars indicate SD. *, $P < 0.05$, as determined by Student's *t* test, in comparison to mock-infected cells (A, E, and F) or to wild-type MEFs (D).

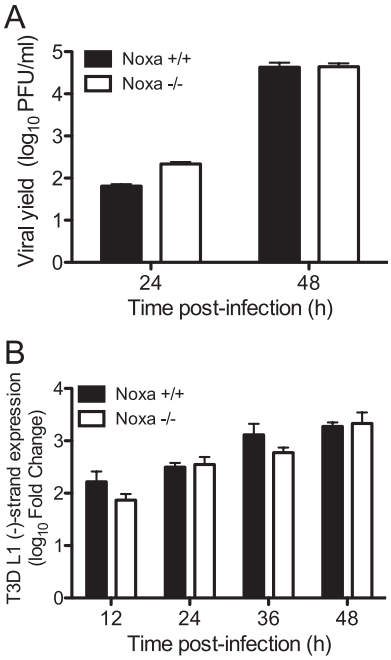

FIG 5 Reovirus replication is not influenced by Noxa expression. (A) Noxa$^{+/+}$ and Noxa$^{-/-}$ MEFs were infected with T3D at an MOI of 1 PFU/cell. Titers of infectious virus in cell lysates at 0, 24, and 48 h postinfection were determined by a plaque assay. The results are expressed as viral yields for triplicate samples. (B) Noxa$^{+/+}$ and Noxa$^{-/-}$ MEFs were infected with T3D at an MOI of 100 PFU/cell. Levels of T3D L1 minus-strand RNA at the indicated times were quantified by using qPCR and normalized to GAPDH expression levels. The results are expressed as the $\log_{10}$ mean fold increases in L1 minus-strand levels relative to the levels at the time of infection for two independent experiments with duplicate samples. The error bars indicate SD.

focused on the transcription factors IRF-3 and NF-κB, which play central roles in the antiviral innate immune response. Both are required to elicit the type I IFN response, and both are linked to apoptosis induction following viral infection. Here, we show that these roles are distinct, as IFN induction and signaling are not required for apoptosis induced by reovirus infection. Additionally, we identify a role for Noxa, a proapoptotic member of the Bcl-2 family, in mediating apoptosis following reovirus infection. Noxa induction is dependent on IRF-3 and NF-κB, suggesting that these transcription factors function to integrate both cellular antiviral and apoptotic responses.

IRF-3 and NF-κB are activated as early as 2 to 4 h following reovirus infection (20, 34, 35), and ISGs are upregulated by 6 to 12 h postinfection (58). In contrast, despite its dependence on IRF-3 and NF-κB, we did not observe a strong increase in Noxa expression levels, particularly in MEFs, until 24 h postinfection, with the most marked upregulation at 36 and 48 h postinfection. This find-

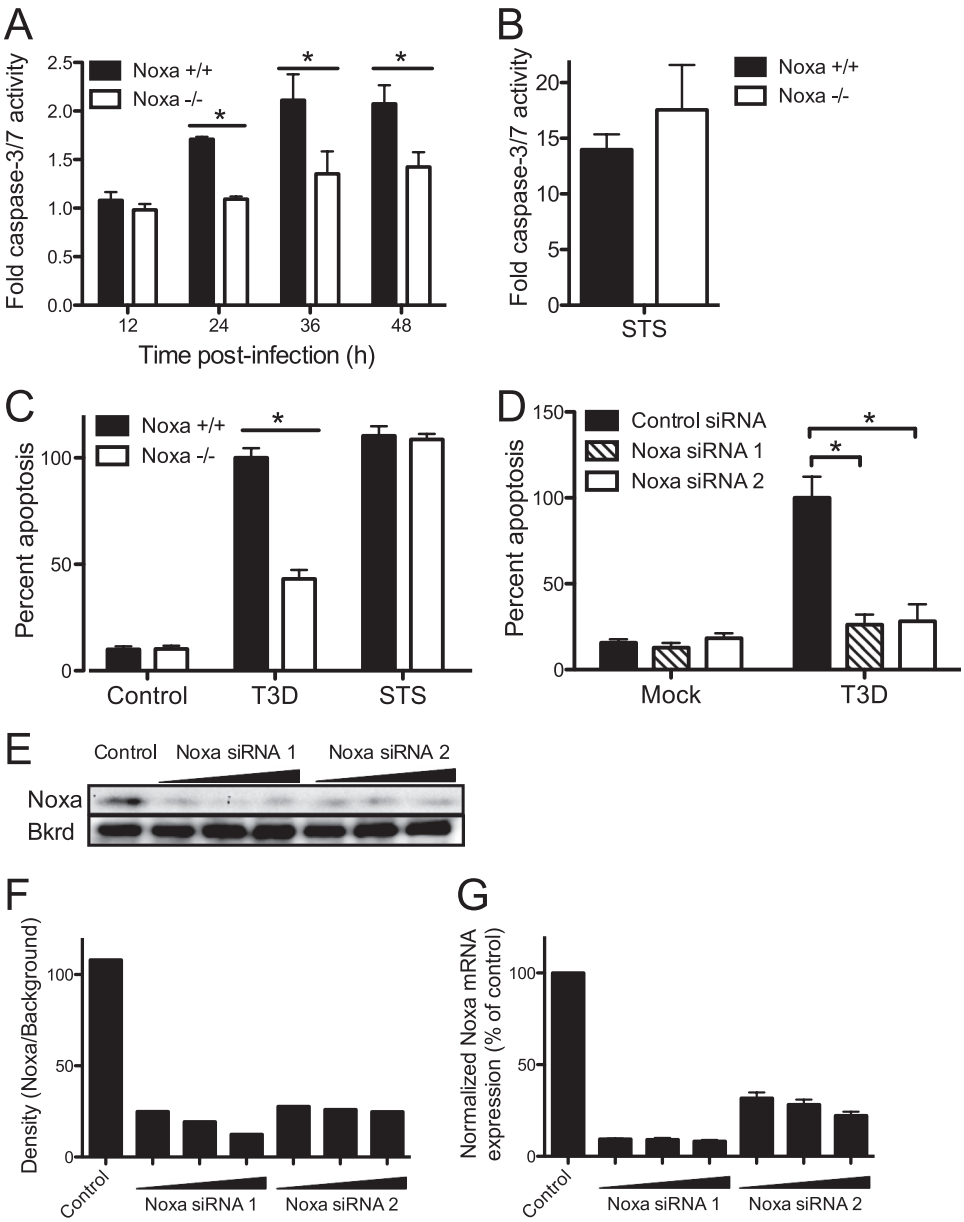

FIG 6 Noxa is required for maximum induction of apoptosis by reovirus. (A) Noxa$^{+/+}$ MEFs and Noxa$^{-/-}$ MEFs were mock infected, infected with T3D at an MOI of 100 PFU/cell (A), or treated with STS (B). Caspase-3/7 activity in cell lysates was determined at the indicated times postinfection. Caspase-3/7 activity in cell lysates from STS-treated cells was determined at 5 h posttreatment. The results are expressed as the mean ratios of caspase-3/7 activity from infected cell lysates to that from mock-infected cells for triplicate samples. The error bars indicate SD. (C) Noxa$^{+/+}$ MEFs and Noxa$^{-/-}$ MEFs were mock infected, infected with T3D at an MOI of 100 PFU/cell, or treated with STS. The percentage of apoptotic cells was determined after staining with acridine orange at 48 h postinfection and 16 h posttreatment. The results are expressed as the mean percentages of apoptotic cells for triplicate samples, normalized to the average percentage of apoptotic cells in T3D-infected Noxa$^{+/+}$ MEFs. The error bars indicate SD. (D) 293T cells were transfected twice with a control siRNA or Noxa-specific siRNAs and infected with T3D at an MOI of 100 PFU/cell. The percentage of apoptotic cells was determined after staining with acridine orange at 48 h postinfection. The results are expressed as the mean percentages of apoptotic cells for triplicate samples, normalized to the average percentage of apoptotic cells in T3D-infected, control siRNA-transfected cells. (E to G) Noxa expression following siRNA treatment was quantified by the immunoblotting of transfected cell lysates with an antiserum specific for Noxa (E and F) and qPCR analysis of total mRNA extracted from transfected cells using Noxa-specific primers (G). Noxa protein levels were quantified by using densitometry and normalized to the intensity of a nonspecific background band (Bkrd) (F). Noxa mRNA levels were normalized to GAPDH and expressed as the percentage of Noxa expression relative to that of control siRNA-transfected cells (G). The error bars indicate SD. *, $P < 0.05$, as determined by Student's *t* test, in comparison to Noxa$^{+/+}$ MEFs (A and C) or control siRNA transfection (D).

ing is consistent with data from microarray experiments examining cellular gene expression following reovirus infection up to 24 h postinfection, in which alterations in Noxa expression were not observed (27, 58, 64, 75). However, the timing of Noxa upregulation following reovirus infection is distinct from that observed following ECMV, Sendai virus, and VSV infections, in which Noxa induction occurs within 3 to 8 h postinfection (45, 81). There are several possible explanations for the delay between

reovirus-induced transcription factor activation and Noxa upregulation. IRF-3 and NF-κB may require a prolonged association with the Noxa promoter before observable Noxa induction can been found. Alternatively, a transcriptional repressor may have to be removed from the Noxa promoter, which might occur only following prolonged infection. Although binding sites for both IRF-3 and NF-κB have been identified in the Noxa promoter (32, 37, 45, 60), its induction may also require the activities of other transcription factors that are induced only at late times postinfection. One such possibility is IRF-1, which transactivates the Noxa promoter following infection by Sendai virus and VSV (45) and is upregulated by reovirus in primary cardiac myocytes (3). As cellular transcriptional activity in response to reovirus infection is dynamic (16, 17), the precise molecular regulation of Noxa expression may reflect the changing transcriptional state of infected cells. Nonetheless, the delay in Noxa upregulation may function as a late response to persistent viral replication. If type I IFNs are insufficient to inhibit the virus, then perhaps Noxa upregulation, which commits the cell to apoptosis, functions as a final antiviral response.

In mammalian cell cultures, Noxa expression, and, therefore, increased levels of apoptosis, did not alter reovirus replication. This observation is consistent with many reports of the relationship between apoptosis and reovirus replicative capacity. Reovirus replication is not altered or only modestly dampened in the presence or absence of proapoptotic proteins, including Bid (24), IRF-3 (35), and NF-κB (20). Additionally, inhibitors of apoptosis induction do not alter reovirus replication (25). However, in animal models, these proteins do alter reovirus replication in an organ-specific context (24, 36, 57). Importantly, IRF-3 and NF-κB have roles in IFN induction, which also limits viral replication, making it difficult to make unambiguous conclusions about the role of apoptosis in reovirus replication *in vivo*. However, both Bid-deficient mice and caspase-3-deficient mice exhibit decreased reovirus replication in the CNS (7, 24). Similarly, a reovirus mutant that displays normal replication but a reduced capacity to induce apoptosis in cultured cells produces lower yields in the CNS of infected mice (22). Together, these results suggest that apoptosis is required for efficient replication *in vivo*. Whether Noxa has a role in reovirus replication and pathogenesis in infected animals remains to be determined.

A Noxa deficiency did not lead to the complete inhibition of apoptosis, as approximately 50% of Noxa$^{-/-}$ MEFs were apoptotic following reovirus infection. These results indicate that Noxa is not absolutely required for reovirus apoptosis but instead contributes to the efficiency of the proapoptotic stimulus. Similar results were observed previously for other proteins known to play a role in reovirus apoptosis, including IRF-3 (35) and NF-κB p50 (20). Reovirus induces multiple apoptotic signals in host cells, including components of both the extrinsic (15, 16, 18) and intrinsic (42, 43) apoptotic pathways. Taken together, these results suggest that cells have multiple redundant mechanisms for initiating cell death following virus infection. The removal of any of the upstream components of these pathways can alter the efficiency of cell death but is unlikely to completely abrogate the response. Since apoptosis is a primary component of the pathogenesis of reovirus infection in the CNS (55) and heart (28, 57), and the inhibition of these pathways was suggested previously to be a possible therapeutic strategy for viral encephalitis and myocarditis (6, 28, 66), these results suggest that interventions must be targeted at later events in apoptosis induction, such as caspase-3 activation, for full efficacy.

Two other proteins involved in intrinsic apoptotic pathways are implicated in cell death following reovirus infection. Bax, a proapoptotic Bcl-2 family member that engages Bak to form the mitochondrial apoptosis-inducing channel in the outer mitochondrial membrane, interacts directly with a novel BH3 domain in IRF-3 (12). Importantly, Bax is essential for apoptosis induced by dsRNA (12), but the role of Bax in reovirus-induced apoptosis is not completely understood. In cultured cells, reovirus apoptosis occurs independently of Bax and Bak, as levels of apoptosis in MEFs lacking Bax and Bak are equivalent to those in wild-type cells (89). However, in Bax-deficient mice, reovirus produces less apoptosis and tissue damage in the CNS than those observed for wild-type mice (9). This effect is organ specific, as levels of apoptosis in the heart do not differ between wild-type and Bax-deficient animals. Thus, Bax may function to induce apoptosis following reovirus infection only in certain cell types or tissues. Given the observed link between Bax and IRF-3, these results may also account for the tissue-specific differences in virus-induced apoptosis observed for IRF-3-deficient mice (36).

A second such molecule is the BH3-only protein Bid, which activates the mitochondrion-based apoptotic amplification loop following death receptor signaling (46). Bid is cleaved by activated caspase-8 to form tBid, which alters the permeability of the outer mitochondrial membrane to release cytochrome *c* and induce the intrinsic apoptotic pathway. Bid is cleaved following reovirus infection and is required for reovirus-induced apoptosis (24). Bid cleavage during reovirus infection requires NF-κB and appears to occur after the activation of TRAIL receptor (TRAIL-R), as cleavage does not occur in TRAIL-R-deficient MEFs (24). The mechanism by which NF-κB modulates TRAIL or TRAIL-R following reovirus infection is not clear. Although there is evidence for an NF-κB-dependent induction of TRAIL, DR4, and DR5 (52, 67, 72, 73), there is substantial evidence that NF-κB protects cells from TRAIL-dependent apoptosis (4, 10, 41, 44). The latter observations are substantiated by experiments with reovirus, which suggested that NF-κB activation must be inhibited prior to TRAIL-dependent cell death (16). One possible explanation for these disparate results is the involvement of the NF-κB c-Rel subunit, which modulates the expression of TRAIL receptors, in opposition to p65/RelA (14, 65). c-Rel is activated following reovirus infection, although its role in reovirus-induced apoptosis has not been defined (34). How these pathways synergize with the NF-κB-dependent induction of Noxa, and whether IRF-3 is also involved, remains to be determined.

Noxa was first linked to p53-dependent apoptosis following genotoxic stress (56, 74, 87). NF-κB is implicated in the p53-dependent induction of Noxa (1, 60), suggesting that it coordinates transcriptional responses to DNA damage. Analyses of gene expression patterns following reovirus infection indicated an upregulation of genes involved in cellular DNA damage responses (27, 58). Additionally, reovirus infection inhibits cell cycle progression at the G_2/M checkpoint via an unknown mechanism involving viral nonstructural protein σ1s (62, 63). Given the importance of p53 in cell cycle regulation and the known activation of NF-κB following reovirus infection, we think that it is possible that interactions between the NF-κB and p53 pathways resulting in Noxa induction couple DNA damage and apoptosis induction.

The precise coordination of innate immune signaling and programmed cell death pathways is essential for mounting effective cellular defenses against viral infections. Ideally, cellular antiviral responses would be sufficient to limit virus replication. However, if a virus evades the antiviral state and continues to replicate, cells must be prepared to undergo apoptosis to mitigate the tissue damage caused by infection. We found that the transcription factors IRF-3 and NF-κB, which are activated by PRRs early in infection, function as central integrators of these responses during reovirus infection. Both factors are required for the induction of type I IFNs and the generation of an antiviral state. In a separate and distinct pathway, these factors also sensitize infected cells to the induction of apoptosis through the upregulation of the BH3-only protein Noxa. The upregulation of Noxa occurs only at late times postinfection, suggesting that it functions as a final attempt to limit virus replication prior to the cessation of cellular activity. It would also provide a means of facilitating the immune clearance of infected cells. Much remains to be determined about the regulation of these pathways, including the mechanisms of feedback inhibition of apoptotic processes following the successful induction of an antiviral state and the role of Noxa in reovirus infection *in vivo*. However, given the critical functions of apoptosis in reovirus encephalitis and myocarditis (26, 55), the NF-κB- and IRF-3-dependent induction of Noxa is likely to play an important role in the pathogenesis of reovirus infection.

ACKNOWLEDGMENTS

We thank members of our laboratories for many helpful discussions and Yosune Camio, John Parker, Andrea Pruijssers, and Yevangelina Rybak for technical assistance, reagents, and advice.

This research was supported by Public Health Service awards F32 AI071440 (G.H.H.), R15 AI094440 (G.H.H.), and R01 AI50080 (T.S.D.) and the Elizabeth B. Lamb Center for Pediatric Research. Additional support was provided by Public Health Service awards P30 CA68485 for the Vanderbilt-Ingram Cancer Center and P60 DK20593 for the Vanderbilt Diabetes Research and Training Center and the Colgate University Core Incentive Program and Student Diversity Research Initiative. We have no financial conflicts of interest.

REFERENCES

1. **Aleyasin H, et al.** 2004. Nuclear factor-κB modulates the p53 response in neurons exposed to DNA damage. J. Neurosci. **24**:2963–2973.
2. **Andersen J, VanScoy S, Cheng T-F, Gomez D, Reich NC.** 2007. IRF-3-dependent and augmented target genes during viral infection. Genes Immun. **9**:168–175.
3. **Azzam-Smoak K, Noah DL, Stewart MJ, Blum MA, Sherry B.** 2002. Interferon regulatory factor-1, interferon-beta, and reovirus-induced myocarditis. Virology **298**:20–29.
4. **Baetu TM, Kwon H, Sharma S, Grandvaux N, Hiscott J.** 2001. Disruption of NF-κB signaling reveals a novel role for NF-κB in the regulation of TNF-related apoptosis-inducing ligand expression. J. Immunol. **167**: 3164–3173.
5. **Balachandran S, et al.** 2000. Alpha/beta interferons potentiate virus-induced apoptosis through activation of the FADD/caspase-8 death signaling pathway. J. Virol. **74**:1513–1523.
6. **Beckham JD, Goody RJ, Clarke P, Bonny C, Tyler KL.** 2007. Novel strategy for treatment of viral central nervous system infection utilizing a cell-permeating inhibitor of c-Jun N-terminal kinase. J. Virol. **81**: 6984–6992.
7. **Beckham JD, Tuttle KD, Tyler KL.** 2010. Caspase-3 activation is required for reovirus-induced encephalitis in vivo. J. Neurovirol. **16**:306–317.
8. **Beg A, Baltimore D.** 1996. An essential role for NF-κB in preventing TNF-α-induced cell death. Science **274**:782–784.
9. **Berens HM, Tyler KL.** 2011. The proapoptotic Bcl-2 protein Bax plays an important role in the pathogenesis of reovirus encephalitis. J. Virol. **85**: 3858–3871.
10. **Bernard D, Quatannens B, Vandenbunder B, Abbadie C.** 2001. Rel/NF-κB transcription factors protect against tumor necrosis factor (TNF)-related apoptosis-inducing ligand (TRAIL)-induced apoptosis by upregulating the TRAIL decoy receptor DcR1. J. Biol. Chem. **276**: 27322–27328.
11. **Chakrabarti A, Jha BK, Silverman RH.** 2011. New insights into the role of RNase L in innate immunity. J. Interferon Cytokine Res. **31**:49–57.
12. **Chattopadhyay S, et al.** 2010. Viral apoptosis is induced by IRF-3-mediated activation of Bax. EMBO J. **29**:1762–1773.
13. **Chawla-Sarkar M, et al.** 2003. Apoptosis and interferons: role of interferon-stimulated genes as mediators of apoptosis. Apoptosis **8**:237–249.
14. **Chen X, Kandasamy K, Srivastava RK.** 2003. Differential roles of RelA (p65) and c-Rel subunits of nuclear factor κB in tumor necrosis factor-related apoptosis-inducing ligand signaling. Cancer Res. **63**:1059–1066.
15. **Clarke P, et al.** 2000. Reovirus-induced apoptosis is mediated by TRAIL. J. Virol. **74**:8135–8139.
16. **Clarke P, Meintzer SM, Moffitt LA, Tyler KL.** 2003. Two distinct phases of virus-induced nuclear factor kappa B regulation enhance tumor necrosis factor-related apoptosis-inducing ligand-mediated apoptosis in virus-infected cells. J. Biol. Chem. **278**:18092–18100.
17. **Clarke P, Debiasi RL, Meintzer SM, Robinson BA, Tyler KL.** 2005. Inhibition of NF-kappa B activity and cFLIP expression contribute to viral-induced apoptosis. Apoptosis **10**:513–524.
18. **Clarke P, Beckham JD, Leser JS, Hoyt CC, Tyler KL.** 2009. Fas-mediated apoptotic signaling in the mouse brain following reovirus infection. J. Virol. **83**:6161–6170.
19. **Coffey MC, Strong JE, Forsyth PA, Lee PW.** 1998. Reovirus therapy of tumors with activated Ras pathway. Science **282**:1332–1334.
20. **Connolly JL, et al.** 2000. Reovirus-induced apoptosis requires activation of transcription factor NF-κB. J. Virol. **74**:2981–2989.
21. **Danthi P, Hansberger MW, Campbell JA, Forrest JC, Dermody TS.** 2006. JAM-A-independent, antibody-mediated uptake of reovirus into cells leads to apoptosis. J. Virol. **80**:261–1270.
22. **Danthi P, et al.** 2008. Reovirus apoptosis and virulence are regulated by host cell membrane penetration efficiency. J. Virol. **82**:161–172.
23. **Danthi P, Coffey CM, Parker JSL, Abel TW, Dermody TS.** 2008. Independent regulation of reovirus membrane penetration and apoptosis by the μ1 φ domain. PLoS Pathog. **4**:e1000248.
24. **Danthi P, et al.** 2010. Bid regulates the pathogenesis of neurotropic reovirus. PLoS Pathog. **6**:e1000980.
25. **Debiasi RL, et al.** 1999. Reovirus-induced apoptosis is preceded by increased cellular calpain activity and is blocked by calpain inhibitors. J. Virol. **73**:695–701.
26. **DeBiasi RL, Edelstein C, Sherry BB, Tyler KL.** 2001. Calpain inhibition protects against virus-induced apoptotic myocardial injury. J. Virol. **75**: 351–361.
27. **DeBiasi RL, et al.** 2003. Reovirus-induced alteration in expression of apoptosis and DNA repair genes with potential roles in viral pathogenesis. J. Virol. **77**:8934–8947.
28. **DeBiasi RL, et al.** 2004. Caspase inhibition protects against reovirus-induced myocardial injury in vitro and in vivo. J. Virol. **78**:11040–11050.
29. **Duncan MR, Stanish SM, Cox DC.** 1978. Differential sensitivity of normal and transformed human cells to reovirus infection. J. Virol. **28**: 444–449.
30. **Eitz Ferrer P, et al.** 2011. Induction of Noxa-mediated apoptosis by modified vaccinia virus Ankara depends on viral recognition by cytosolic helicases, leading to IRF-3/IFN-β-dependent induction of pro-apoptotic Noxa. PLoS Pathog. **7**:e1002083.
31. **Furlong DB, Nibert ML, Fields BN.** 1988. Sigma 1 protein of mammalian reoviruses extends from the surfaces of viral particles. J. Virol. **62**: 246–256.
32. **Goubau D, et al.** 2009. Transcriptional re-programming of primary macrophages reveals distinct apoptotic and anti-tumoral functions of IRF-3 and IRF-7. Eur. J. Immunol. **39**:527–540.
33. **Grandvaux N, et al.** 2002. Transcriptional profiling of interferon regulatory factor 3 target genes: direct involvement in the regulation of interferon-stimulated genes. J. Virol. **76**:5532–5539.
34. **Hansberger MW, et al.** 2007. IκB kinase subunits α and γ are required for activation of NF-κB and induction of apoptosis by mammalian reovirus. J. Virol. **81**:1360–1371.

35. **Holm GH, et al.** 2007. Retinoic acid-inducible gene-I and interferon-b promoter stimulator-1 augment proapoptotic responses following mammalian reovirus infection via interferon regulatory factor-3. J. Biol. Chem. **282**:21953–21961.
36. **Holm GH, et al.** 2010. Interferon regulatory factor 3 attenuates reovirus myocarditis and contributes to viral clearance. J. Virol. **84**:6900–6908.
37. **Inta I, et al.** 2006. Bim and noxa are candidates to mediate the deleterious effect of the NF-κB subunit RelA in cerebral ischemia. J. Neurosci. **26**: 12896–12903.
38. **Kato H, et al.** 2006. Differential roles of MDA5 and RIG-I helicases in the recognition of RNA viruses. Nature **441**:101–105.
39. **Kawai T, et al.** 2005. IPS-1, an adaptor triggering RIG-I- and Mda5-mediated type I interferon induction. Nat. Immunol. **6**:981–988.
40. **Kayagaki N, et al.** 1999. Type I interferons (IFNs) regulate tumor necrosis factor-related apoptosis-inducing ligand (TRAIL) expression on human T cells: a novel mechanism for the antitumor effects of type I IFNs. J. Exp. Med. **189**:1451–1460.
41. **Kim YS, Schwabe RF, Qian T, Lemasters JJ, Brenner DA.** 2002. TRAIL-mediated apoptosis requires NF-kappaB inhibition and the mitochondrial permeability transition in human hepatoma cells. Hepatology **36**: 1498–1508.
42. **Kominsky DJ, Bickel RJ, Tyler KL.** 2002. Reovirus-induced apoptosis requires mitochondrial release of Smac/DIABLO and involves reduction of cellular inhibitor of apoptosis protein levels. J. Virol. **76**:11414–11424.
43. **Kominsky DJ, Bickel RJ, Tyler KL.** 2002. Reovirus-induced apoptosis requires both death receptor- and mitochondrial-mediated caspase-dependent pathways of cell death. Cell Death Differ. **9**:926–933.
44. **Kreuz S, Siegmund D, Scheurich P, Wajant H.** 2001. NF-κB inducers upregulate cFLIP, a cycloheximide-sensitive inhibitor of death receptor signaling. Mol. Cell. Biol. **21**:3964–3973.
45. **Lallemand C, et al.** 2006. Single-stranded RNA viruses inactivate the transcriptional activity of p53 but induce NOXA-dependent apoptosis via post-translational modifications of IRF-1, IRF-3 and CREB. Oncogene **26**:328–338.
46. **Li H, Zhu H, Xu CJ, Yuan J.** 1998. Cleavage of BID by caspase 8 mediates the mitochondrial damage in the Fas pathway of apoptosis. Cell **94**: 491–501.
47. **Libermann TA, Baltimore D.** 1990. Activation of interleukin-6 gene expression through the NF-kappaB transcription factor. Mol. Cell. Biol. **10**:2327–2334.
48. **Loo YM, et al.** 2008. Distinct RIG-I and MDA5 signaling by RNA viruses in innate immunity. J. Virol. **82**:335–345.
49. **Lu M, Liao F.** 2011. Interferon-stimulated gene ISG12b2 is localized to the inner mitochondrial membrane and mediates virus-induced cell death. Cell Death Differ. **18**:925–936.
50. **Lu R, Au WC, Yeow WS, Hageman N, Pitha PM.** 2000. Regulation of the promoter activity of interferon regulatory factor-7 gene. Activation by interferon and silencing by hypermethylation. J. Biol. Chem. **275**: 31805–31812.
51. **McAllister CS, Samuel CE.** 2009. The RNA-activated protein kinase enhances the induction of interferon-β and apoptosis mediated by cytoplasmic RNA sensors. J. Biol. Chem. **284**:1644–1651.
52. **Mendoza FJ, Ishdorj G, Hu X, Gibson SB.** 2008. Death receptor-4 (DR4) expression is regulated by transcription factor NF-κB in response to etoposide treatment. Apoptosis **13**:756–770.
53. **Meylan E, et al.** 2005. Cardif is an adaptor protein in the RIG-I antiviral pathway and is targeted by hepatitis C virus. Nature **437**:1167–1172.
54. **Muller U, et al.** 1994. Functional role of type I and type II interferons in antiviral defense. Science **264**:1918–1921.
55. **Oberhaus SM, Smith RL, Clayton GH, Dermody TS, Tyler KL.** 1997. Reovirus infection and tissue injury in the mouse central nervous system are associated with apoptosis. J. Virol. **71**:2100–2106.
56. **Oda E, et al.** 2000. Noxa, a BH3-only member of the Bcl-2 family and candidate mediator of p53-induced apoptosis. Science **288**:1053–1058.
57. **O'Donnell SM, et al.** 2005. Organ-specific roles for transcription factor NF-κB in reovirus-induced apoptosis and disease. J. Clin. Invest. **115**: 2341–2350.
58. **O'Donnell SM, et al.** 2006. Identification of an NF-κB-dependent gene network in cells infected by mammalian reovirus. J. Virol. **80**:1077–1086.
59. **Ohyama K, Sano T, Toyoda H.** 2004. Predominant contribution of IFN-β expression to apoptosis induction in human uterine cervical fibroblast cells by influenza-virus infection. Biol. Pharm. Bull. **27**:1750–1757.
60. **O'Prey J, et al.** 2010. p53-mediated induction of Noxa and p53AIP1 requires NFkappaB. Cell Cycle **9**:947–952.
61. **Pindel A, Sadler A.** 2011. The role of protein kinase R in the interferon response. J. Interferon Cytokine Res. **31**:59–70.
62. **Poggioli GJ, Keefer CJ, Connolly JL, Dermody TS, Tyler KL.** 2000. Reovirus-induced G2/M cell cycle arrest requires σ1s and occurs in the absence of apoptosis. J. Virol. **74**:9562–9570.
63. **Poggioli GJ, Dermody TS, Tyler KL.** 2001. Reovirus-induced σ1s-dependent G2/M cell cycle arrest results from inhibition of p34cdc2. J. Virol. **75**:7429–7434.
64. **Poggioli GJ, et al.** 2002. Reovirus-induced alterations in gene expression related to cell cycle regulation. J. Virol. **76**:2585–2594.
65. **Ravi R, et al.** 2001. Regulation of death receptor expression and TRAIL/Apo2L-induced apoptosis by NF-kappaB. Nat. Cell Biol. **3**:409–416.
66. **Richardson-Burns SM, Tyler KL.** 2005. Minocycline delays disease onset and mortality in reovirus encephalitis. Exp. Neurol. **192**:331–339.
67. **Rivera-Walsh I, Waterfield M, Xiao G, Fong A, Sun SC.** 2001. NF-kappaB signaling pathway governs TRAIL gene expression and human T-cell leukemia virus-I Tax-induced T-cell death. J. Biol. Chem. **276**: 40385–40388.
68. **Sato M, et al.** 2000. Distinct and essential roles of transcription factors IRF-3 and IRF-7 in response to viruses for IFN-alpha/beta gene induction. Immunity **13**:539–548.
69. **Schiff LA, Nibert ML, Tyler KL.** 2007. Orthoreoviruses and their replication, p 1853–1916. *In* Knipe DM et al. (ed), Fields virology, 5th ed, vol 2. Lippincott Williams & Wilkins, Philadelphia, PA.
70. **Selleri C, et al.** 1997. Involvement of Fas-mediated apoptosis in the inhibitory effects of interferon-alpha in chronic myelogenous leukemia. Blood **89**:957–964.
71. **Seth RB, Sun L, Ea CK, Chen ZJ.** 2005. Identification and characterization of MAVS, a mitochondrial antiviral signaling protein that activates NF-κB and IRF3. Cell **122**:669–682.
72. **Shetty S, et al.** 2002. Tumor necrosis factor-related apoptosis inducing ligand (TRAIL) up-regulates death receptor 5 (DR5) mediated by NFκB activation in epithelial derived cell lines. Apoptosis **7**:413–420.
73. **Shetty S, et al.** 2005. Transcription factor NF-kappaB differentially regulates death receptor 5 expression involving histone deacetylase 1. Mol. Cell. Biol. **25**:5404–5416.
74. **Shibue T, et al.** 2003. Integral role of Noxa in p53-mediated apoptotic response. Genes Dev. **17**:2233–2238.
75. **Smith JA, et al.** 2006. Reovirus induces and benefits from an integrated cellular stress response. J. Virol. **80**:2019–2033.
76. **Smith RE, Zweerink HJ, Joklik WK.** 1969. Polypeptide components of virions, top component and cores of reovirus type 3. Virology **39**: 791–810.
77. **Stawowczyk M, Van Scoy S, Kumar KP, Reich NC.** 2011. The interferon stimulated gene 54 promotes apoptosis. J. Biol. Chem. **286**:7257–7266.
78. **Stoeckel J, Hay JG.** 2006. Drug evaluation: reolysin—wild-type reovirus as a cancer therapeutic. Curr. Opin. Mol. Ther. **8**:249–260.
79. **Strasser A.** 2005. The role of BH3-only proteins in the immune system. Nat. Rev. Immunol. **5**:189–200.
80. **Sumpter RJ, et al.** 2005. Regulating intracellular antiviral defense and permissiveness to hepatitis C virus RNA replication through a cellular RNA helicase, RIG-I. J. Virol. **79**:2689–2699.
81. **Sun Y, Leaman DW.** 2005. Involvement of Noxa in cellular apoptotic responses to interferon, double-stranded RNA, and virus infection. J. Biol. Chem. **280**:15561–15568.
82. **Takaoka A, Yanai H.** 2006. Interferon signalling network in innate defence. Cell. Microbiol. **8**:907–922.
83. **Tanaka N, et al.** 1998. Type I interferons are essential mediators of apoptotic death in virally infected cells. Genes Cells **3**:29–37.
84. **Toth AM, Devaux P, Cattaneo R, Samuel CE.** 2009. Protein kinase PKR mediates the apoptosis induction and growth restriction phenotypes of C protein-deficient measles virus. J. Virol. **83**:961–968.
85. **Twigger K, et al.** 2008. Enhanced in vitro and in vivo cytotoxicity of combined reovirus and radiotherapy. Clin. Cancer Res. **14**:912–923.
86. **Tyler KL, et al.** 1995. Differences in the capacity of reovirus strains to induce apoptosis are determined by the viral attachment protein σ1. J. Virol. **69**:6972–6979.
87. **Villunger A, et al.** 2003. p53- and drug-induced apoptotic responses mediated by BH3-only proteins Puma and Noxa. Science **302**: 1036–1038.
88. **Virgin HW, IV, Bassel-Duby R, Fields BN, Tyler KL.** 1988. Antibody

protects against lethal infection with the neurally spreading reovirus type 3 (Dearing). J. Virol. **62**:4594–4604.
89. **Wisniewski ML, et al.** 2011. Reovirus infection or ectopic expression of outer capsid protein μ1 induces apoptosis independently of the cellular proapoptotic proteins Bax and Bak. J. Virol. **85**:296–304.
90. **Xu LG, et al.** 2005. VISA is an adapter protein required for virus-triggered IFN-b signaling. Mol. Cell **19**:727–740.
91. **Yoneyama M, et al.** 2004. The RNA helicase RIG-I has an essential function in double-stranded RNA-induced innate antiviral responses. Nat. Immunol. **5**:730–737.
92. **Zhang P, Samuel CE.** 2007. Protein kinase PKR plays a stimulus- and virus-dependent role in apoptotic death and virus multiplication in human cells. J. Virol. **81**:8192–8200.
93. **Zhao W, et al.** 2008. A conserved IFN-alpha receptor tyrosine motif directs the biological response to type I IFNs. J. Immunol. **180**: 5483–5489.